Published in final edited form as:

Cancer Prev Res (Phila). 2016 May ; 9(5): 339–348. doi:10.1158/1940-6207.CAPR-15-0348.

Obesity-associated alterations in inflammation, epigenetics and mammary tumor growth persist in formerly obese mice

Emily L. Rossi[1], **Rebecca E. de Angel**[2], **Laura W. Bowers**[1], **Subreen A. Khatib**[1], **Laura A. Smith**[1], **Eric Van Buren**[3], **Priya Bhardwaj**[4], **Dilip Giri**[5], **Marcos R. Estecio**[6], **Melissa A. Troester**[7], **Brionna Y. Hair**[7], **Erin L. Kirk**[7], **Ting Gong**[6], **Jianjun Shen**[6], **Andrew J. Dannenberg**[4], and **Stephen D. Hursting**[1,2]

[1]Department of Nutrition, University of North Carolina, Chapel Hill, NC 27599

[2]Department of Nutritional Sciences, University of Texas, Austin, TX 78712

[3]Department of Biostatistics, University of North Carolina, Chapel Hill, NC 27599

[4]Department of Medicine, Weill Cornell Medical College, New York, NY 10065

[5]Department of Pathology, Memorial Sloan-Kettering Cancer Center, New York, NY 10065

[6]Department of Epigenetics and Molecular Carcinogenesis, University of Texas MD Anderson Cancer Center, Houston, TX 77030

[7]Department of Epidemiology, University of North Carolina, Chapel Hill, NC 27599

Abstract

Using a murine model of basal-like breast cancer, we tested the hypothesis that chronic obesity, an established breast cancer risk and progression factor in women, induces mammary gland epigenetic reprogramming and increases mammary tumor growth. Moreover, we assessed whether the obesity-induced epigenetic and protumor effects are reversed by weight normalization. Ovariectomized female C57BL/6 mice were fed a control diet or diet-induced obesity (DIO) regimen for 17 weeks, resulting in a normal weight or obese phenotype, respectively. Mice on the DIO regimen were then randomized to continue the DIO diet or were switched to the control diet, resulting in formerly obese (FOb) mice with weights comparable to control mice. At week 24, all mice were orthotopically injected with MMTV-Wnt-1 mouse mammary tumor cells. Mean tumor volume, serum IL-6 levels, expression of pro-inflammatory genes in the mammary fat pad, and mammary DNA methylation profiles were similar in DIO and FOb mice, and higher than in controls. Many of the genes found to have obesity-associated hypermethylation in mice were also found to be hypermethylated in the normal breast tissue of obese versus non-obese human subjects, and nearly all of these concordant genes remained hypermethylated after significant weight loss in the FOb mice. Our findings suggest that weight normalization may not be sufficient to reverse the effects of chronic obesity on epigenetic reprogramming and inflammatory signals in the microenvironment that are associated with breast cancer progression.

Corresponding Author: Stephen D. Hursting, Ph.D., Department of Nutrition CB #7461, The University of North Carolina, Chapel Hill, NC 27599, Tel. +1 919 966-7346, Fax: 919 966-7215, hursting@email.unc.edu.

Conflict of interest: The authors disclose no potential conflicts of interest.

Keywords

Wnt-1 mouse model; inflammation and tumor development; DNA methylation/epigenetics; breast cancer; obesity

Introduction

Obesity is highly prevalent in the United States and many other parts of the world and is an established risk and progression factor for several intrinsic subtypes of breast cancer, including basal-like breast cancer (BLBC), in postmenopausal women (1). Greater rates of metastatic breast cancer and increased mortality are seen in the obese breast cancer patient population, independent of disease stage at diagnosis (2, 3). These effects may be mediated in part by adipose tissue inflammation, as excess adipose tissue results in local as well as systemic effects. Obesity is typically accompanied by increased systemic levels of pro-inflammatory mediators, such as interleukin-6 (IL-6), tumor necrosis factor alpha (TNFα), matrix metalloproteinase-9 (MMP-9) and interleukin-1 beta (IL-1β), and these can independently influence tumor growth. In addition, obesity enhances the secretion of monocyte chemoattractant protein-1 (MCP-1), which stimulates the recruitment of macrophages to adipose tissue, including the breast adipose. These tumor-associated macrophages likely contribute to tumor growth by increasing local and/or systemic inflammatory and angiogenic factors and generating reactive oxygen species (4, 5).

In obese mice, calorie restriction reduces mammary tissue expression of several mediators of inflammation including TNFα and IL-1β (6). Less is known about the effects of obesity or weight loss interventions on the epigenome. There is mounting evidence that DNA methylation can be affected by energy balance. For example, weight loss interventions (30% energy reduction) in obese male subjects have been shown to induce DNA methylation changes at the TNFα promoter after only 8 weeks of diet intervention (7). In another study, severe weight loss after gastric bypass surgery in obese humans normalized methylation in the promoter regions of 11 out of 14 metabolic genes that had been dysregulated by obesity (8). Expression of the EZH2 gene, which encodes the epigenetic regulator histone-lysine-N-methyltransferase, has been linked to breast cancer growth and metastasis (9). It is also modulated in the offspring of obese mothers (10), suggesting that this enzyme may mediate some of the effects of energy balance on epigenetic regulation. Although DNA methylation patterns are energy responsive, the relationship between weight loss, aberrant DNA methylation, adipose tissue inflammation, and cancer progression are unknown.

Epidemiological and preclinical studies have clearly shown that the metabolic perturbations typically accompanying obesity promote breast cancer progression (11). One study in particular illustrated how women who underwent bariatric surgery had a 5% reduction in incidence of breast cancer after 5 years of follow up from surgery compared to women who did not undergo a weight loss intervention- surgical or otherwise (12). However, with the exception of bariatric surgery interventions, the impact of intentional obesity reversal prior to diagnosis has not been well-established. The epidemiologic data have been mixed regarding non-surgically induced weight loss, reflecting the difficulties in achieving and

maintaining meaningful weight loss. Despite their limitations, animal model studies may be informative in addressing this question given their benefit of greater control of diet, physical activity and numerous other confounding variables. Sundaram et al. (2014) found that a high-fat diet promotes mammary tumor progression in a transgenic mouse model of BLBC, and switching mice to a low-fat diet after a short-term high-fat diet exposure led to small but statistically significant weight loss and reversed many of the high-fat diet effects on tumor progression to that of control levels (13). However, the transgenic mouse model used in this study were resistant to obesity induction, and tumors arose early in life, so the question of whether the mammary tumor-promoting effects of chronic obesity are reversed by weight loss was not addressed. We have previously found in a mouse model of chronic obesity, as well as in clinical studies of obese women, that a severe weight loss intervention may provide an anti-cancer benefit, but moderate weight loss had minimal effects on cancer-related biomarkers in mice and women and tumor growth in mice (14, 15).

Given the uncertainty regarding the benefits of obesity reversal, we sought to determine the effects of weight loss on the host microenvironment and tumor progression in an orthotopic transplant model of murine BLBC in syngeneic mice. Here we demonstrate that tumor growth did not change with significant weight loss prior to orthotopic tumor transplant, despite the normalization of several obesity-related hormones. Moreover, we provide evidence that breast tumor growth after obesity reversal may be driven by epigenetic dysregulation in the microenvironment as well as sustained elevations in inflammatory signaling. These findings suggest that short-term weight loss may not reverse the tumor-promoting epigenetic reprogramming and increased inflammatory signaling that accompanies chronic obesity.

Materials and Methods

Mice and Diets

All animal protocols were approved by the University of Texas at Austin Institutional Animal Care and Use Committee (IACUC) and carried out in compliance with all guidelines and regulations. Six-week-old female ovariectomized C57BL/6 mice were obtained from Charles River Laboratories, Inc. (Frederick, MD), individually housed on a 12-hour light/dark cycle, and consumed food and water *ad libitum*. Food intake was measured twice a week and body weights were measured weekly. Mice were randomized to continue on the control diet (n=17) or a 60% kcal from fat diet-induced obesity (DIO) diet regimen (n=34; D12492, Research Diets, Inc.). After 17 weeks on diet, the DIO mice were randomized to either continue on the DIO regimen (DIO, n=17) or switch to the control diet to induce gradual weight loss; this latter group is referred to as formerly obese (FOb, n=17). After 24 weeks on diet, 5 mice per group were fasted for 6–8 hours and then euthanized for pre-tumor tissue collection. The remaining mice (n=15/group) were orthotopically injected with 5×10^4 syngeneic viable MMTV-Wnt-1 mammary tumor cells as previously described (16). *In vivo* growth was measured twice/week with skinfold calipers, and *in vivo* tumor area was approximated using the formula πr^2. At study endpoint (week 36), mice were euthanized and mammary tumors, tumor-adjacent and tumor-distal mammary fat pad were excised and divided in portions to be formalin fixed or flash frozen in liquid nitrogen and stored at

−80°C until further analysis. Mice were excluded if they had developed dermatitis during study (one DIO mouse and one FOb mouse). *Ex vivo* tumor volume was calculated using the formula $4/3\pi \times R_1^2 \times R^2$, (with R1 denoting the smaller radius of the ellipsoid) (17).

Quantitative Magnetic Resonance Analysis

Body composition was measured on all mice at weeks 17 and 24 of diet treatments by quantitative magnetic resonance (qMR) (Echo Medical Systems, Houston, TX). Measurements included lean mass, fat mass and total water mass. Percent body fat was calculated by dividing fat mass by total body weight.

Serum Hormone, Cytokine and Adipokine Measurement

Serum was collected from mice fasted 6–8 hours, prior to tumor cell injection (week 24) by retro-orbital bleed. Serum hormones, adipokines, and cytokines, including leptin, adiponectin, insulin, and IL-6, were measured using mouse adipokine LINCOplex®Multiplex Assays (Millipore, Inc., Billerica, MA) and analyzed on a BioRad Bioplex 200 analysis system (Biorad, Inc., Hercules, CA). Insulin-like growth factor 1 (IGF-1) concentrations were measured using a Millipore Milliplex Rat/Mouse IGF-1 Single Plex assay (Millipore, Inc.).

Crown-like Structure Analysis

Four micron-thick sections were prepared from formalin-fixed, paraffin-embedded mammary fat pad tissue and stained with hematoxylin and eosin. The total number of CLS per section was quantified by a pathologist, blind to the sample group, and the amount of adipose tissue present on each slide was determined using NIH Image J. Prevalence of CLS was quantified as CLS per cm^2 of adipose tissue.

Quantification of Adipocyte Infiltration in Tumor Tissue

Four micron-thick sections were prepared from formalin-fixed, paraffin-embedded tumor tissue and stained with hematoxylin and eosin. Tumors were chosen at random (4–5/group) and digitally imaged under 20× magnification. The total number of adipocytes per section (2–4 representative sections, each 830 μm × 580 μm) was quantified independently by 3 investigators who were blinded to experimental group.

Quantitative RT-PCR

Total RNA was extracted from the flash-frozen tumor-adjacent and tumor-distal mammary fat pad samples collected at end of study using TRI-Reagent (Sigma-Aldrich, St.Louis, MO) according to manufacturer's instructions. RNA concentration was spectrophotometrically determined using a nanodrop (Thermo Scientific, Logan, UT) and quality was confirmed using an Agilent 2100 Bioanalyzer (Santa Clara, CA). RNA was reverse transcribed with Multiscribe RT (Applied Biosystems, Carlsbad, CA). Resulting cDNA from tissue samples were assayed in triplicate for PCR using Taqman® Gene Expression Assays for IL-6, TNFα, MMP-9, IL-1β, IGFBP6, CITED1, TFE3, JAK3, EZH2, SMYD3, and TSC22D3 (Applied Biosystems). PCR reactions were completed using a ViiATM7 Real time PCR system

(Applied Biosciences). Gene expression data were normalized to the housekeeping gene β-actin and analyzed using the delta delta cycle threshold method (18).

Methylation Analysis

DNA was extracted from the 9th tumor-distal mammary fat pad, at end of study (n=3/group) using UltraPure™ Phenol:Chloroform:Isoamyl Alcohol per manufacturer's instructions (Life Technologies, Carlsbad, CA). Genome-wide methylation profiles for mammary fat pad from control, DIO and FOb mice were determined by RRBS (Reduced Representation Bisulfite Sequencing). Among the available methods for genome-wide analysis of the DNA methylation, we selected RRBS based in its compatibility and validation with mouse DNA, its capacity to investigate individual sites by bisulfite-sequencing, and the large number (above 400 thousand) of CpG sites that are evaluated in a single experiment. Library preparation and sequencing were completed at the UT MD Anderson Cancer Center's DNA Methylation Analysis Core and Science Park Next-Generation Sequencing Facility, according to published protocols (19, 20) (Supplementary Table S3). Briefly, 1ug of genomic DNA was digested with MspI, a methylation-insensitive enzyme that cleaves the DNA at CCGG sequences, followed by end-repair, A-tailing and size selection. Enrichment for CpG sites in CG-dense and CpG islands is achieved by selective collection and PCR amplification of MspI fragments with sizes between 40bp and 170bp.Sequence reads were mapped to the mouse genome (mm10) using Bismark bisulfite read mapper. The location of individual CpG sites in relationship to known genes was based on the mm10 RefSeq gene annotations and classified as promoter (CpG sites 1 kb upstream of the annotated transcription start site (TSS) and extending 500 base pairs downstream of TSS), exon, intron, or CpG island. CpG island coordinates were collected from the UCSC Genome Browser mm10 version, Genome Reference Consortium GRCm38. Differential methylation was calculated by filtering samples based on read coverage ≥ 20, then performed at the single base level independent of the CpG site location. TSS of transcripts smaller than 300 bp were removed for the analysis. Methylkit R package was used to apply logistic regression and the likelihood ratio test. Observed p-values were adjusted with the success likelihood index method (SLIM).

Selection of Samples from the Normal Breast Study for Methylation Analysis

Selection criteria for the Normal Breast Study included having an invasive ductal carcinoma with a tissue specimen sampled ≥4 cm from tumor margins, undergoing reduction mammoplasty, or undergoing prophylactic surgery (21). There were 150 participants with invasive breast cancer had tissue collected that was >4 cm from the tumor. Participants were randomly selected from each BMI group: 30 from the high BMI (>30), 20 from the normal BMI (25–30), and 22 from the low BMI (<25) group. All prophylactics and reduction participants were also included. In all, 96 participants were selected. All tissue specimens were snap frozen. A 50 mg sample was taken from the participants' tissue specimens and used for methylation assessment. The University of North Carolina at Chapel Hill Institutional Review Board approved this study.

DNA Extraction from Human Breast Samples

DNA was isolated using the DNeasy Blood and Tissue kit from Qiagen (Venlo, Netherlands) following the manufacturer's protocol. Sodium bisulfite modification of the DNA was conducted using EZ DNA Methylation Gold Kit (Zymo Research, Orange, CA), and 500 ng of DNA was used for the HumanMethylation450 BeadChip platform. The samples were processed for DNA methylation analysis by the University of North Carolina at Chapel Hill's Mammalian Genotyping Core.

Concordance Between Mouse and Human Genes Methylated in Response to Energy Balance Modulation

We compared our mouse methylation dataset with a dataset obtained from the University of North Carolina Normal Breast Study utilizing non-tumorous breast tissue, subject to methylation array and stratified by BMI. A methylation difference was calculated for each significant methylation change (obese vs. non-obese) with a positive coefficient signifying increasing methylation with increased adiposity. Intraspecies concordance was assayed only for genes with significant differences within species (Supplementary Table S2). Welch's t-test was used for the pairwise comparisons between obese and non-obese humans using R version 3.1.2 (http://www.r-project.org). Comparisons between both species was done by one-way analysis of variance (ANOVA) using GraphPad Prism V6 with Bonferroni correction for multiple comparisons.

Statistical Analysis

Values are presented as mean ± standard deviation (SD). One-way ANOVA using Tukey's multiple comparisons correction was used to assess the effects of diet treatment on body weight and fat percentage, mean tumor size, serum hormone and cytokine concentrations, and mammary fat pad gene expression. Student's t-test was used to compare differences in CLS between experimental groups and control. For all tests, GraphPad Prism software was used (GraphPad Software Inc., La Jolla, CA), and $P \leq 0.05$ was considered statistically significant.

Results

Body Weight and Body Composition of Control, DIO, and FOb mice

Mice were fed a low-fat control or a diet-induced obesity (DIO) regimen for 17 weeks, at which time percent body fat, assessed by quantitative resonance analysis, was higher in DIO mice (59.7 ± 1.8%) compared to control mice (39.5 ± 4.0%) ($P < 0.001$; Fig. 1A). DIO mice also had a higher mean body weight (51.5 ± 0.7 g) than control mice (33.1 ± 0.7 g) (Fig. 1B). After weight loss was initiated at week 17, FOb mice lost 27.6 ± 3.4% of their body weight (14.2 ± 1.7 g) ($P < 0.0001$) relative to their last weight taken while on the DIO diet. By week 24, the body fat percentage in FOb mice (45.1 ± 3.5%) did not significantly differ from mice maintained on the control diet throughout study (42.6 ± 3.3%), with DIO mice (60.1 ± 1.5%) having significantly greater body fat percentage than control and FOb mice ($P < 0.001$; Fig. 1A). FOb and control mice maintained significantly lower body weights than DIO mice through the end of study ($P < 0.0001$, Fig. 1B).

Effect of Weight Loss on Serum Metabolic and Inflammatory Markers

Serum was collected from mice at week 24 by retro-orbital bleed, prior to tumor cell injection and when the body weights of the FOb mice were statistically equivalent to the control mice. The reduction in adiposity in the FOb mice was accompanied by lower serum leptin ($P < 0.0001$), leptin:adiponectin ratio ($P < 0.0001$), and insulin ($P < 0.0001$) relative to DIO mice (Fig. 1C–E), with concentrations statistically equivalent to those found in the control mice. IGF-1 levels were significantly higher in DIO mice relative to control ($P < 0.05$; Fig. 1G) but were intermediate in FOb mice and not statistically different from the levels seen in control or DIO mice. Furthermore, IL-6 levels did not differ between FOb and DIO mice and were significantly elevated in both groups compared to control mice ($P < 0.05$; Fig. 1H).

Weight Loss in FOb Mice Reduced Prevalence of Crown-like Structures (CLS)

The high-fat dietary regimen increased the prevalence of CLS (expressed as CLS / area of tissue in cm^2) in the mammary fat pad of DIO mice relative to control mice ($P < 0.003$; Fig. 2). This was analyzed in tissue harvested at the interim (week 24) time point. FOb mice had a significant reduction in CLS compared to DIO mice ($P < 0.03$); however, prevalence of CLS remained slightly elevated relative to control, though this difference was not statistically significant ($P = 0.4$).

Weight Loss in FOb Mice Does Not Decrease Basal-like Mammary Tumor Burden

Ex vivo tumor volume from DIO and FOb mice were larger (1792.7± 1132.9 mm^3, 1563.4 ± 1673.3 mm^3, respectively) than tumors from the control mice (51.6 ± 139.8 mm^3) ($P < 0.05$; Fig. 3A). Furthermore, a shared attribute of tumors from both the DIO and FOb groups were the presence of adipose cells infiltrating the tumor in greater number compared to control (Fig. 3B). Tumors from DIO mice contained a significantly higher number of adipocytes than control tumors (168.4 ± 83.4 adipocytes / mm^2 and 34.6 ± 32.2 adipocytes / mm^2, respectively; $P < 0.05$). Tumors in FOb mice had an intermediate level of adipocyte infiltration (127.1 ± 83.6 adipocytes/mm^2) that did not significantly differ from either control ($P = 0.19$) or DIO ($P = 0.66$). Collectively, these findings suggest that significant weight loss does not completely reverse the effects of obesity on BLBC growth and adipocyte-infiltration.

Pro-Inflammatory Cytokine Gene Expression is Elevated in Mammary Fat Pad from FOb Mice

RT-PCR analysis was performed on tumor-distal mammary fat pad (n=4–5 mice). Relative to control, FOb mice had significantly elevated IL-6 expression ($P < 0.001$, Fig. 4A), with DIO mice having non-significantly elevated levels relative to control. TNFα expression was significantly elevated in DIO ($P < 0.04$) and FOb ($P < 0.03$; Fig 4B) versus control mice. MMP-9 expression was greater in FOb mice ($P < 0.05$; Fig. 4C), with DIO mice experiencing an intermediate increase compared to control. IL1-® expression was significantly higher in FOb and DIO mice ($P < 0.01$; Fig. 4D) compared to control.

Weight Loss Fails to Normalize Obesity-induced Hypermethylation Patterns and Histone Methyltransferase Enzymes EZH2 and SMYD3 in Mammary Fat Pad

To determine whether the sustained elevation in tumor growth observed in FOb mice may be mediated in part by epigenetic reprogramming in the microenvironment, we assessed the global DNA methylation pattern of the tumor-distal mammary fat pad at end of study. DIO mice had 39 genes significantly hypermethylated compared to control. Of these 39 differentially methylated genes, FOb mice generally possessed intermediate levels of methylation relative to control and DIO mice, suggesting that weight reduction back to control levels was insufficient to completely reverse the epigenetic reprogramming that occurs with chronic obesity (Fig. 5A). FOb mice had 11 genes significantly hypermethylated compared to control. While the methylation levels of these genes were also elevated in DIO mice, they were not significantly different from control

Hypermethylated genes in DIO and FOb mice relative to control were entered into Qiagen's Ingenuity® Pathway Analysis (IPA) to delineate pathological signaling pathways. Gene expression was confirmed on a select number of genes (Fig. 5B–H). IPA Biofunction analysis connected the genes from our methylation analysis to a disease or biological function. Cancer was the primary disease with 23 genes hypermethylated in DIO (22 of the genes) or DIO and FOb (1 gene) implicated in cancer, specifically neoplasia of epithelial tissue (Supplementary Table S1). Another biofunction with 17 genes associated with it was cellular growth and proliferation. Four genes in our data set were identified as playing a role in cell-mediated immune response. Significant overlap of differentially methylated genes in DIO or FOb mice with each biofunction was determined by Fisher's exact test.

We moved forward with genes that appeared in the IPA Biofunction of cancer with a function of neoplasia of epithelial tissue (IGFBP6, SMYD3, and JAK3) and transcription factor TSC22D3 and investigated their role as regulators in inflammatory signaling, with particular interest in the relationship between each gene and IL-6 (Supplementary Figure S1) As stated previously, IL-6 serum (Fig. 1H) and tumor-distal mammary fat pad mRNA levels (Fig. 4A) were elevated in DIO and FOb mice relative to controls. Of note, inhibitors of IL-6 including TSC22D3 (intron) and JAK3 (exon) were hypermethylated. EZH2 was also predicted by the IPA analysis to be regulated by these genes, and expression of EZH2 in tumor-distal mammary fat pad of endpoint animals was significantly higher in DIO ($P < 0.05$) and FOb ($P < 0.005$) mice compared to control mice (Fig. 5H). The gene for another methyltransferase enzyme, SET and MYND domain-containing protein 3 (SMYD3), was also identified as differentially methylated in our analysis, and its expression in tumor-distal mammary fat pad was significantly elevated in FOb mice ($P < 0.02$), with DIO mice having non-significantly elevated levels.

Hypermethylation Concordance in Mammary Tissue from Non-obese and Obese Humans and Mice

After we identified a panel of genes that were significantly hypermethylated in the mammary fat pad of DIO mice compared to controls, we assessed the methylation status of this gene panel in a methylation data set from normal human breast tissue involving subjects stratified by body mass index (BMI) (Supplementary Table S2). Thirteen genes were

identified with concordant hypermethylation (% methylation difference with the same directionality) in DNA from normal mammary tissue at the same genomic feature (i.e. intron vs. exon) in obese vs. non-obese women and mice (Table 1). However, as some significant methylation changes mapped to the same gene, of the 13 concordant genes, 6 had additional discordant methylation sites. We also identified an additional 3 genes with only discordant methylation between species. We then compared methylation (as % methylated DNA) for CpG's related to the same gene in the same genomic feature (i.e. intron or exon) between women and mice. Non-obese women and control fed mice had levels of DNA methylation that were statistically equivalent for 4 of the 13 concordant genes identified. Of the 13 hypermethylated genes in obese women and DIO mice, 6 genes reached statistical equivalence (CDK2AP1, CYFIP1, MAF, MAML3, SH3PXD2A, SMYD3). Of those 4 were statistically equivalent in obese women, DIO mice, and FOb mice. Seven genes were significantly different between obese humans and DIO mice due to varying degrees of hypermethylation.

Discussion

In our orthotopic tumor transplant model of BLBC in C57BL/6 mice, we found that DIO, relative to control diet, elevated: a) body fat percentage; b) serum leptin, leptin:adiponectin ratio, insulin, IGF-1, and IL-6; c) prevalence of CLS in mammary fat pad; d) mammary tumor growth; and e) genome-wide mammary gland hypermethylation. Significant weight loss initiated after 17 weeks on DIO diet resulted in a normalization of percent body fat and serum leptin, leptin:adiponectin, insulin levels, and prevalence of CLS in mammary fat pad in the FOb mice. Serum IGF-1 decreased to levels intermediate to DIO and control levels. Despite these beneficial metabolic changes and weight normalization, FOb mice had a final tumor volume nearly identical to DIO mice. Additionally, we observed that obesity reversal in the FOb mice failed to normalize serum IL-6 and mammary fat pad inflammatory gene expression as well as aberrant methylation in the mammary gland, and these may contribute to the persistence of the pro-cancer effects of obesity even after weight is normalized. We have identified several genes with concordant obesity-related hypermethylation in humans and mice, and the DNA methylation levels of many of these genes were unchanged after significant weight loss in the FOb mice, providing further support that obesity-associated epigenetic reprogramming may not be easily reversed with weight normalization alone.

To our knowledge, this is the first study to: i) characterize the effects of obesity reversal on mammary gland microenvironment (including DNA methylation) and tumor growth; ii) identify genes with concordant and discordant obesity-related methylation patterns in normal mammary tissue from mice and humans. We and others have previously found that a severe weight loss intervention, or inhibiting the mTOR signaling pathway in obese mice using genetic or pharmacologic approaches (18, 22, 23), decreases murine mammary tumor progression. Severe weight loss in humans, such as that achieved by bariatric surgery, has also shown the ability to significantly decrease inflammatory signaling (24), DNA hypermethylation (8), and cancer risk (12, 25). However, the weight loss that was achieved in our study via an *ad libitum* low-fat diet, which models many human weight loss plans, failed to reduce inflammatory signaling and elevated methylation levels in the FOb mice.

Inflammation is implicated in many of the deleterious effects of obesity (26, 27). In the present study, weight loss in FOb mice normalized metabolic regulators that are elevated in obesity such as serum leptin:adiponectin, insulin, and adipose tissue CLS. However, several measures of inflammation persisted after weight loss, including serum IL-6 and gene expression of inflammatory cytokines in the mammary tissue. Thus, we are able to distinguish the pro-cancer effects of obesity-related metabolic perturbations from obesity-related inflammation, which persists after weight loss.

We also found evidence suggesting that obesity-induced aberrant hypermethylation contributes to the maintenance of a pro-inflammatory, pro-growth microenvironment in the mammary fat pad of mice, and this is not normalized by significant weight loss. Abnormal expression of EZH2 plays a role in cancer growth and metastasis in a variety of cancers, including breast (28). A high-density tissue microarray analysis of breast tumors from 280 patients revealed that EZH2 levels were increased in patients with invasive breast carcinoma relative to patients with no lesions or atypical hyperplasia (29). Additionally, EZH2 increases expression of SMYD3, a histone H3 lysine-4 specific methyltransferase, which plays a key role in the proliferation and migration of several cancers. Cell culture studies have shown that silencing of SMYD3 by siRNA inhibits growth of breast cancer cells (30). We demonstrated here that both EZH2 and SMYD3 expression remained elevated in the mammary fat pad tissue of FOb mice, similar to the DIO group, indicating that these epigenetic regulators may be involved in mediating the mammary tumor-promoting effects of obesity.

Study limitations include the lack of a time course, since it is plausible that FOb mice could have had decreased tumor growth if challenged after a longer period of weight normalization. Additionally, as serum IL-6, mammary fat pad inflammatory gene expression, and mammary fat pad methylation all remained elevated in FOb mice compared to control, we are unable to delineate the individual contribution of each factor to the increased tumor burden. As expected, many but not all methylation changes investigated resulted in a corresponding change in gene expression. This is likely influenced by distance between the site of methylation change and promoter region, influence of chromatin features, or multiple systemic levels of regulation at play (31, 32).

The results of our study raise important questions concerning the relationship between obesity and the progression of more aggressive breast cancers such as the basal type. Numerous studies have shown that obesity is associated with increased risk of mortality from breast cancer (33). As weight loss did not suppress tumor progression in mice that had at one time been obese, further research is needed to investigate a potential critical window regarding the timing and magnitude of weight loss to achieve an anti-tumor effect. Future studies should also explore weight loss in combination with adjuvant therapy, such as prophylactic NSAID use to combat inflammation. The hypermethylation observed in DIO and FOb mice may also provide a new druggable target for breaking the obesity-breast cancer link. In summary, we found that MMTV-Wnt-1 mammary tumor growth was similar in DIO and FOb mice, with both groups exhibiting larger tumors than control mice. DNA methylation in the tumor-distal mammary fat pad at study endpoint was also significantly elevated in DIO mice relative to control, with FOb mice possessing intermediate DNA

methylation levels. This is particularly surprising considering that at the time of tumor cell injection, FOb mice did not differ from control mice in terms of body weight, body composition, and serum metabolic markers of obesity, with the exception of serum IL-6. Taken together, our findings suggest a relationship between chronic obesity, the epigenome, inflammation and mammary cancer. Consequently, a combination of weight loss and epigenetic or anti-inflammatory interventions may be required to effectively break the obesity-breast cancer link.

Supplementary Material

Refer to Web version on PubMed Central for supplementary material.

Acknowledgments

Financial Support: The animal study was supported by Breast Cancer Research Foundation. The mouse methylation analysis was supported by the Science Park NGS Core, supported by CPRIT Core Facility Support Grand RP120348. E.L. Rossi was supported by funds from the University of North Carolina's University Cancer Research Fund. L.W. Bowers was supported by a grant from the National Cancer Institute (R25CA057726).

References

1. Whiteman MK, Hillis SD, Curtis KM, McDonald JA, Wingo PA, Marchbanks PA. Body mass and mortality after breast cancer diagnosis. Cancer Epidemiol Biomarkers Prev. 2005; 14:2009–2014. [PubMed: 16103453]
2. Calle EE, Kaaks R. Overweight, obesity and cancer: epidemiological evidence and proposed mechanisms. Nat Rev Cancer. 2004; 4:579–591. [PubMed: 15286738]
3. Reeves GK, Pirie K, Beral V, Green J, Spencer E, Bull D. Cancer incidence and mortality in relation to body mass index in the Million Women Study: cohort study. BMJ. 2007; 335:1134. [PubMed: 17986716]
4. Sinicrope FA, Dannenberg AJ. Obesity and breast cancer prognosis: weight of the evidence. J Clin Oncol. 2011; 29:4–7. [PubMed: 21115867]
5. Lashinger LM, Ford NA, Hursting SD. Interacting inflammatory and growth signals underlie the obesity-cancer link. J Nutr. 2014; 144:109–113. [PubMed: 24285690]
6. Bhardwaj P, Du B, Zhou XK, Sue E, Harbus MD, Falcone DJ, et al. Caloric restriction reverse obesity induced mammary gland inflammation in mice. Cancer Prev Res (Phila). 2013; 6:282–289. [PubMed: 23430756]
7. Milagro FI, Campión J, Cordero P, Goyenechea E, Gómez-Uriz AM, Abete I, et al. A dual epigenomic approach for the search of obesity biomarkers: DNA methylation in relation to diet-induced weight loss. FASEB J. 2011; 25:1378–1389. [PubMed: 21209057]
8. Barres R, Kirchner H, Rasmussen M, Yan J, Kantor FR, Krook A, et al. Weight loss after gastric bypass surgery in human obesity remodels promoter methylation. Cell Rep. 2013; 25(3):1020–1027. [PubMed: 23583180]
9. Yoo KH, Hennighausen L. EZH2 methyltransferase and H3K27 methylation in breast cancer. International Journal of Biological Sciences. 2012; 8:59–65. [PubMed: 22211105]
10. Borengasser SJ, Kang P, Faske J, Gomez-Acevedo H, Blackburn ML, Badger TM, et al. High fat diet and in utero exposure to maternal obesity disrupts circadian rhythm and leads to metabolic programming of liver in rat offspring. PLoS One. 2014; 9:e84209. [PubMed: 24416203]
11. Hursting SD, Digiovanni J, Dannenberg AJ, Azrad M, Leroith D, Denmark-Wahnefried W, et al. Obesity, Energy Balance and Cancer: *New Opportunities for Prevention*. Cancer Prev Res (Phila). 2012; 5:1260–1272. [PubMed: 23034147]
12. Christou NV, Lieberman M, Sampalis F, Sampalis JS. Bariatric surgery reduces cancer risk in morbidly obese patients. Surg Obes Relat Dis. 2008; 4:691–695. [PubMed: 19026373]

13. Sundaram S, Le TL, Essaid L, Freemerman AJ, Huang MJ, Galanko JA, et al. Weight loss reversed obesity-induced HGF-c-Met pathway and basal-like breast cancer progression. Front Oncol. 2014; 4:175. [PubMed: 25072025]
14. Nogueira LM, Lavigne JA, Chandramouli GV, Lui H, Barrett JC, Hursting SD. Dose-dependent effects of calorie restriction on gene expression, metabolism, and tumor progression are partially mediated by insulin-like growth factor-1. Cancer Med. 2012; 1:275–288. [PubMed: 23342276]
15. Fabian CJ, Kimler BF, Donnelly JE, Sullivan DK, Klemp JR, Petroff BK, et al. Favorable modulation of benign breast tissue and serum risk biomarkers is associated with >10% weight loss in postmenopausal women. Breast Cancer Res Treat. 2013; 142:119–132. [PubMed: 24141897]
16. Nunez NP, Perkins SN, Smith NC, Berrigan D, Berendes DM, Varticovski L, et al. Obesity accelerates mouse mammary tumor growth in the absence of ovarian hormones. Nutr Cancer. 2008; 60:534–541. [PubMed: 18584488]
17. De Angel RE, Blando JM, Hogan MG, Sandoval MA, Lansakara-P DS, Dunlap SM, et al. Stearoyl gemcitabine nanoparticles overcome obesity-induced cancer cell resistance to gemcitabine in a mouse postmenopausal breast cancer model. Cancer Biol Ther. 2013; 14:357–364. [PubMed: 23358472]
18. Nogueira LM, Dunlap SM, Ford NA, Hursting SD. Calorie restriction and rapamycin inhibit MMTV-Wnt-1 mammary tumor growth in a mouse model of postmenopausal obesity. Endocr Relat Cancer. 2012; 19:57–68. [PubMed: 22143497]
19. Gertz J, Varley KE, Reddy TE, Bowling KM, Pauli F, Parker SL, et al. Analysis of DNA methylation in a three-generation family reveals widespread genetic influence on epigenetic regulation. PLoS Genet. 2011; 7:e1002228. [PubMed: 21852959]
20. Gu H, Smith ZD, Bock C, Boyle P, Gnirke A, Meissner A. Preparation of reduced representation bisulfite sequencing libraries for genome-scale DNA methylation profiling. Nat Protoc. 2011; 6:468–481. [PubMed: 21412275]
21. Hair BY, Xu Z, Kirk EL, Harlid S, Sandhu R, Robinson WR, et al. Body mass index associated with genome-wide methylation in breast tissue. Breast Cancer Res Treat. 2015; 151:453–463. [PubMed: 25953686]
22. De Angel RE, Conti CJ, Wheatley KE, Brenner AJ, Otto G, Degraffenried LA, et al. The enhancing effects of obesity on mammary tumor growth and Akt/mTOR pathway activation persist after weight loss and are reversed by RAD001. Mol Carcinog. 2013; 52:446–458. [PubMed: 22290600]
23. Svirshchevskaya EV, Mariotti J, Wright MH, Viskova NY, Telford W, Fowler DH, et al. Rapamycin delays growth of Wnt-1 tumors in spite of suppression of host immunity. BMC Cancer. 2008; 8:176. [PubMed: 18570671]
24. Furet JP, Kong LC, Tap J, Poitou C, Basdevant A, Bouillot JL, et al. Differential adaptation of human gut microbiota to bariatric surgery-induced weight loss: links with metabolic and low-grade inflammation markers. Diabetes. 2010; 59:3049–3057. [PubMed: 20876719]
25. Sjöström L, Narbro K, Sjöström CD, Karason K, Larsson B, Wedel H, et al. Effects of bariatric surgery on mortality in Swedish obese subjects. N Engl J. 2007; 357:741–752.
26. Dandona P, Aljada A, Bandyopadhyay A. Inflammation: the link between insulin resistance, obesity and diabetes. Trends Immunol. 2004; 25:4–7. [PubMed: 14698276]
27. Shoelson, Se; Herrero, L.; Naaz, A. Obesity, inflammation, and insulin resistance. Gastroenterology. 2007; 132:2169–2180. [PubMed: 17498510]
28. Bachmann IM, Halvorsen OJ, Collett K, Stefansson IM, Straume O, Haukaas SA, et al. EZH2 expression is associated with high proliferation rate and aggressive tumor subgroups in cutaneous melanoma and cancers of the endometrium, prostate, and breast. J Clin Oncol. 2006; 24:268–273. [PubMed: 16330673]
29. Kleer CG, Cao Q, Varambally S, Shen R, Ota I, Tomlins SA, et al. EZH2 is a marker of aggressive breast cancer and promotes neoplastic transformation of breast epithelial cells. Proc Natl Acad Sci USA. 2003; 100:11606–11611. [PubMed: 14500907]
30. Hamamoto R, Silva FP, Tsuge M, Nishidate T, Katagiri T, Nakamura Y, et al. Enhanced SMYD3 expression is essential for the growth of breast cancer cells. Cancer Science. 2006; 97:113–118. [PubMed: 16441421]

31. Wagner JR, Busche S, Ge B, Kwan T, Pastinen T, Blanchette M. The relationship between DNA methylation, genetic and expression inter-individual variation in untransformed human fibroblasts. Genome Biol. 2014; 15:R37. [PubMed: 24555846]

32. Jones PA. Functions of DNA methylation: islands, start sites, gene bodies and beyond. Nat Rev Genet. 2012; 13:484–492. [PubMed: 22641018]

33. Chen X, Lu W, Zheng W, Gu K, Chen Z, Zheng Y, et al. Obesity and weight change in relation to breast cancer survival. Breast Cancer Res Treat. 2010; 122:823–833. [PubMed: 20058068]

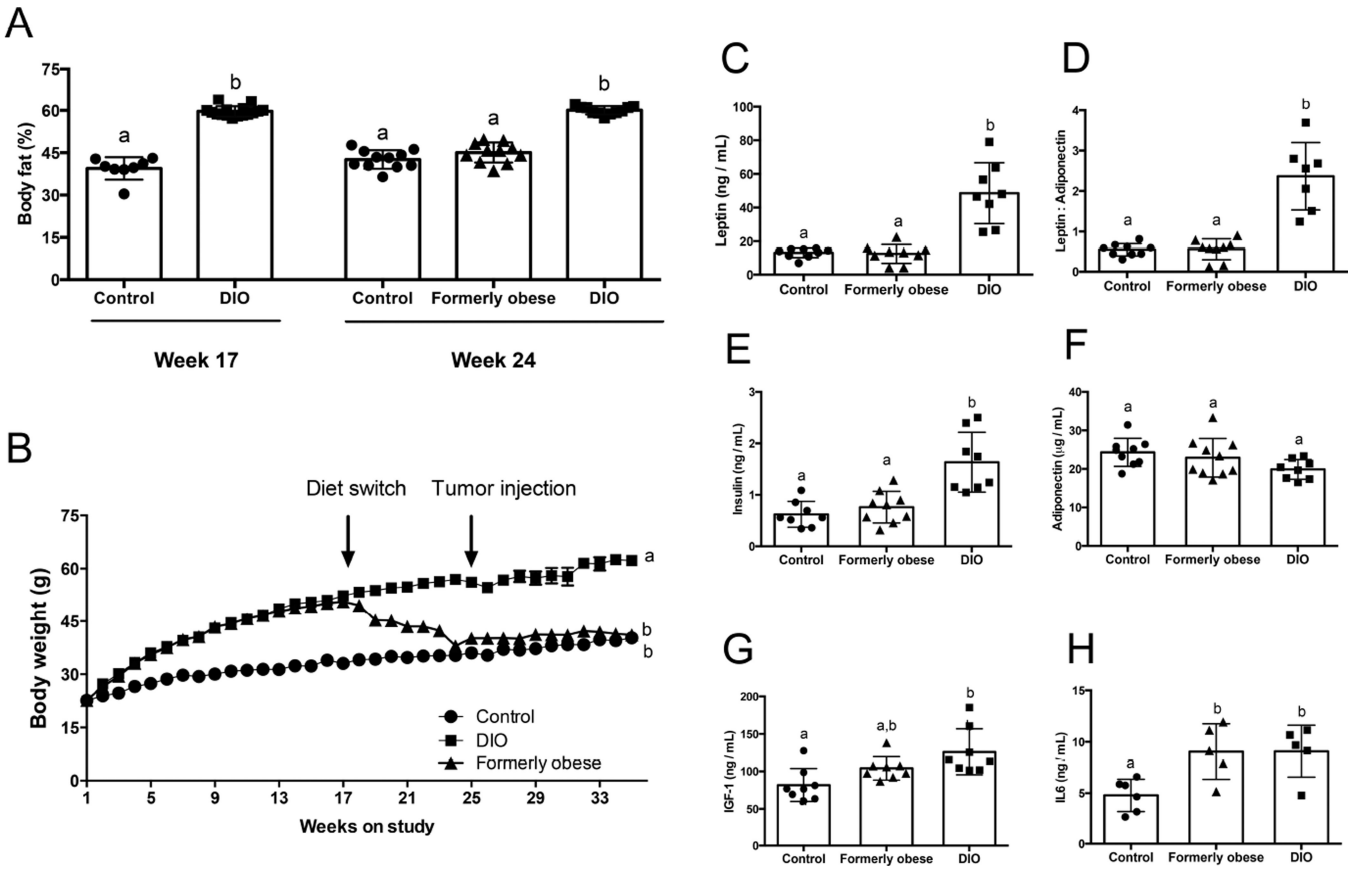

Figure 1.

(A) Percent body fat mass in Control versus Obese mice at Week 17 on diet and in Control, Formerly obese, and Obese mice at Week 24. (B) Body weight in the three diet groups over the course of the study. Different letters indicate significant differences, $P<0.05$. Serum levels of several hormones, growth factors, and adipokines were measured in mice from all three diet groups at Week 24 of study, including (C) leptin, (D) leptin:adiponectin ratio, (E) insulin, (F) adiponectin, (G) IGF-1, (H) IL-6. Different letters indicate significant differences, $P<0.05$.

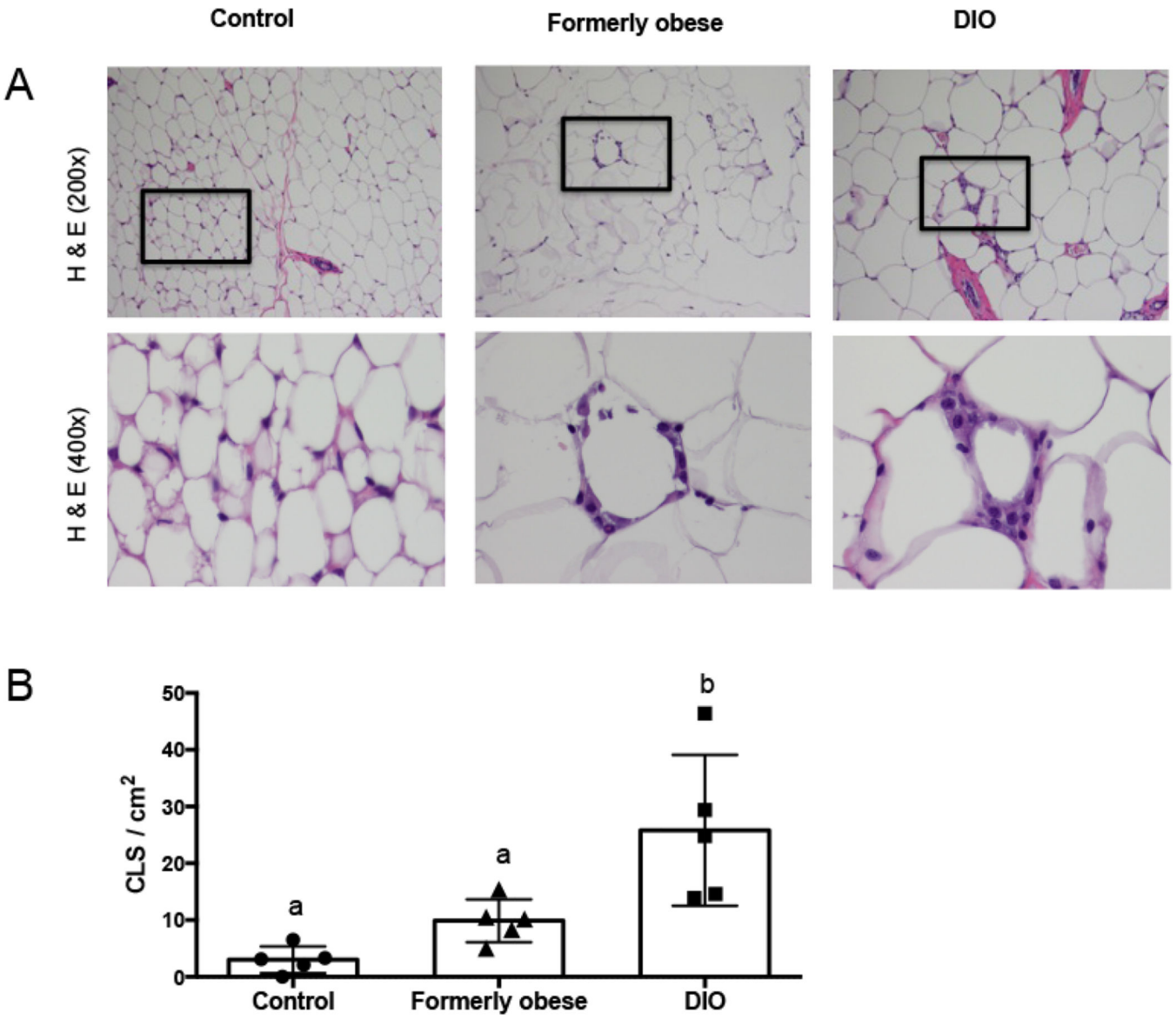

Figure 2.

Mouse mammary fat pad tissue at week 24 on diet was assessed for the prevalence of (A) crown-like structures (CLS) using H & E stained tissue sections, representative image shown. (B) CLS were quantified for each tissue sample as number of CLS per cm^2. Different letters indicate significant differences, $P < 0.05$.

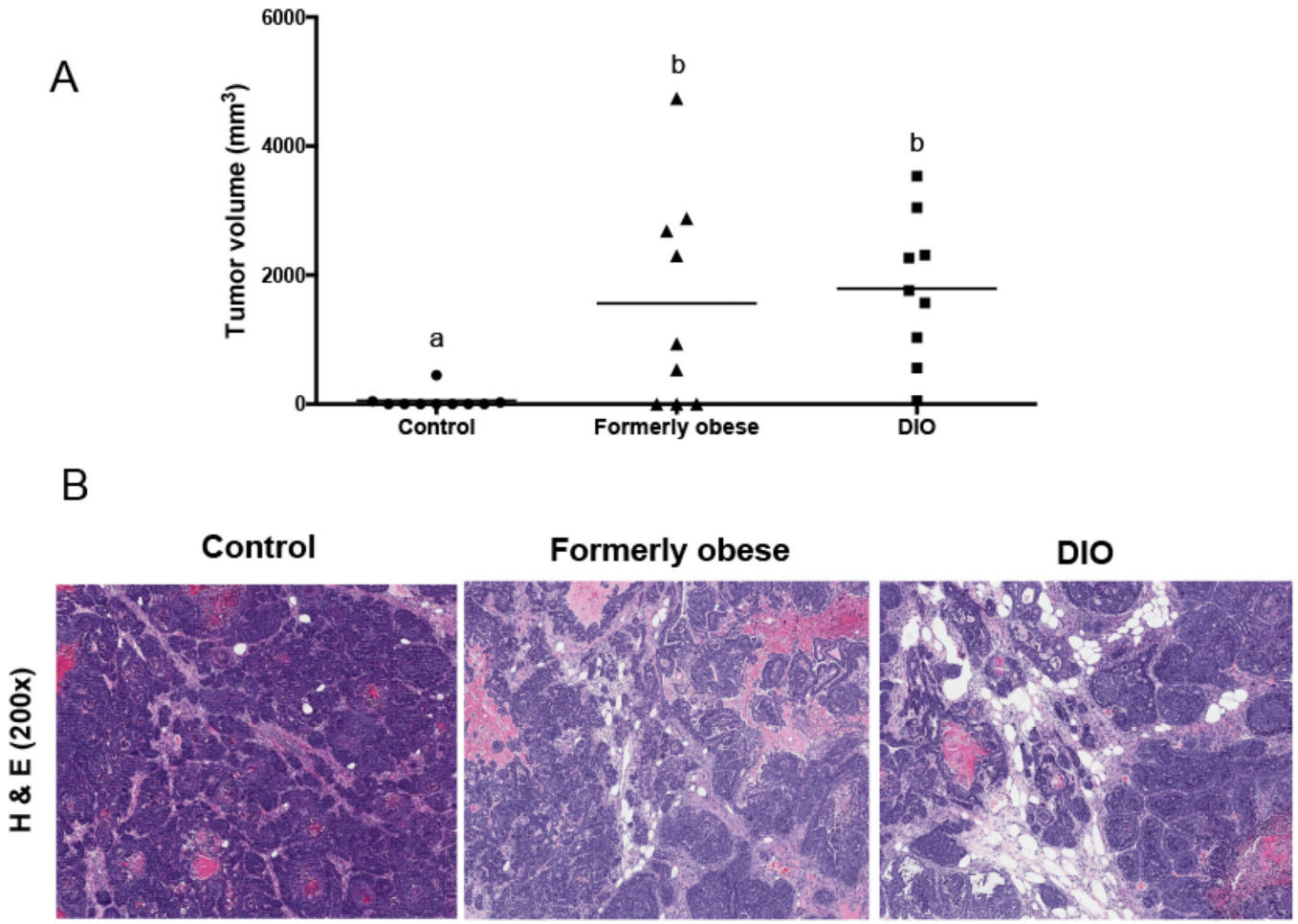

Figure 3.

(A) Ex vivo tumor volume at end of study. (B) Differing levels of adipocyte infiltration into the tumor tissue of mice from the three diet groups. Different letters indicate significant differences, $P < 0.05$.

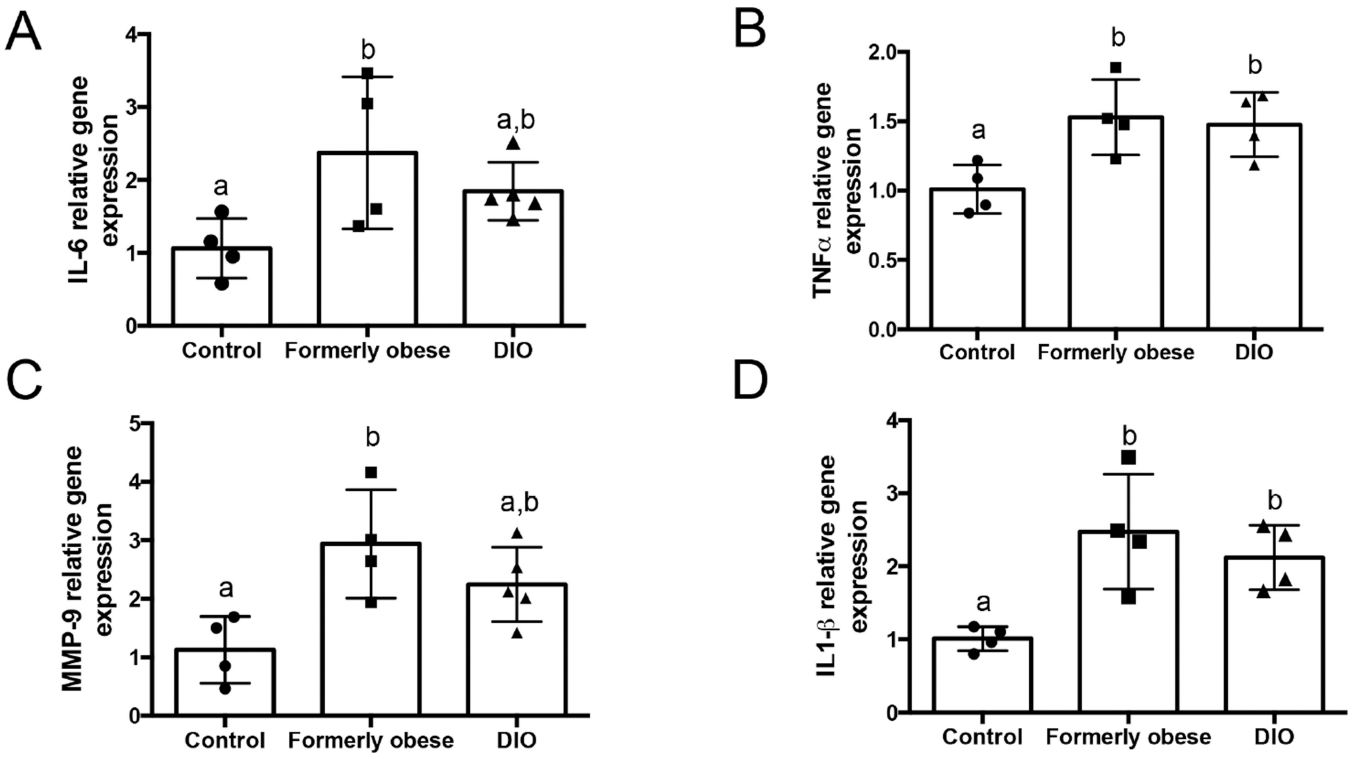

Figure 4.

mRNA expression of pro-inflammatory genes was measured in the tumor-distal mammary fat pad of mice sacrificed at end of study, including (A) IL-6; (B) TNFα; (C) MMP-9; (D) IL-1β. Different letters indicate significant differences, $P < 0.05$.

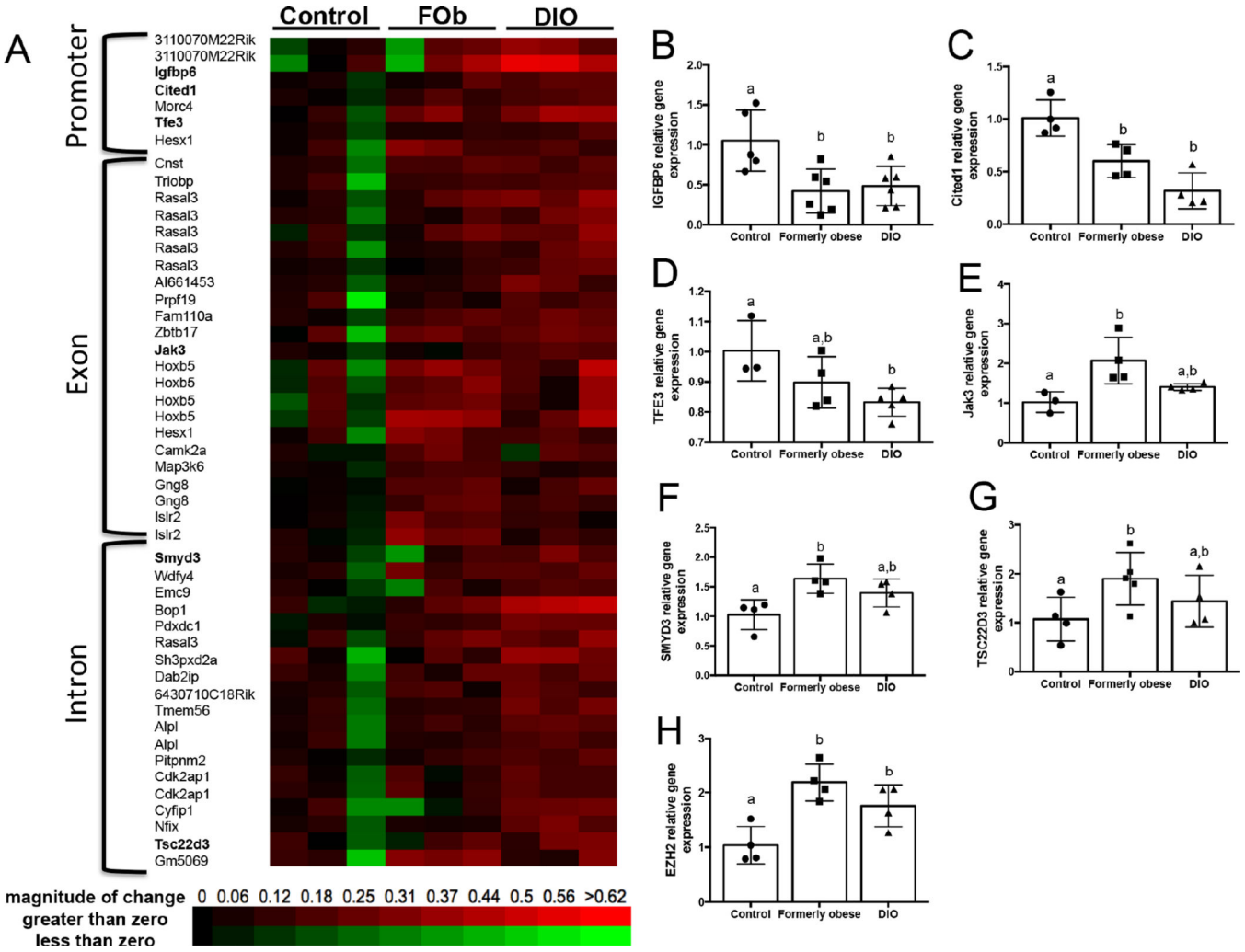

Figure 5.

(A) Heat map representation of gene methylation values expressed as % methylated DNA. Corresponding gene expression of (B) IGFBP6, (C) CITED1, (D) TFE3, (E) JAK3, (F) SMYD3 and (G) TSC22D3 in tumor-distal mammary fat pad. Additional expression shown for implicated genes (H) EZH2. Different letters indicate significant differences, $P < 0.05$.

Table 1

DNA methylation comparisons between obese and non-obese women and DIO, FOb and control mice.

Gene	Chr. Human	Chr. Mouse	Genomic Location	Methylation % Increase In Obesity (Human)	Methylation % Increase In Obesity (Obese Mouse)	Methylation % Increase In Obesity (FOb Mouse)	Human Non-Obese vs. Mouse Control	Human Obese vs. Mouse Obese	Human Obese vs. Mouse FOb
ALPL	chr1:2183 8665	chr4:1377 70933	Intron	**4.25**	35.45	17.92	*P* <0.0001	*P* <0.0001	*P* <0.0001
		chr4:1377 70959	Intron		29.90	14.60	*P* <0.0001	*P* <0.0001	*P* <0.0001
	chr1:2186 8624	chr4:1377 70933	Intron	**5.47**	35.450	17.92	*P* <0.004	*P* <0.0001	*P* <0.0001
		Chr4:1377 70959	Intron		29.90	14.60	*P* <0.001	*P* <0.001	*P* <0.001
CDK2AP1	chr12:123 750864	Chr5:1243 49413	Intron	**5.54**	29.03	13.97	ns	ns	ns
		Chr5:1243 49431	Intron		28.96	19.28	ns	ns	ns
CYFIP1	Chr15:229 211B4	Chr7:5589 1934	Intron	**3.24**	25.64	−3.38	*P* <0.0001	ns	*P* <0.001
ETS1	chr11:128 457459	Chr9:3278 7134	Downstream	**5.42**	29.64	−5.86	ns	*p*<0.001	ns
EXTL3	chr8:2856 0486	chr14:651 11008	Intron	**5.10**	33.38	18.68	*P* <0.01	*P* <0.001	*P* <0.001
FAM110A	Chr20:825 415	Chr2:1519 70815	Exon	**1.49**	25.06	19.17	*P* <0.001	*P* <0.001	*P* <0.001
MAF	chr16:796 38744	chr8:1155 36869	Downstream	**8.65**	16.85	29.12	ns	ns	ns
		chr8:1155 36892	Downstream		12.77	28.26	*P* <0.03	ns	ns
MAML3	chr4:1408 34011	Chr3:5217 1869	Intron	**9.06**	28.02	24.40	ns	ns	ns
	chr4:1408 77994		Intron	**7.72**			ns	*P* <0.0001	*P* <0.0003
	chr4:1409 07113		Intron	**4.49**			*P* <0.0001	ns	ns
	chr4:1410 13584		Intron	**3.21**			*P* <0.0001	*P* <0.0001	*P* <0.0001
PITPNM2	chr12:123 579358	chr5:1241 85502	Intron	**3.83**	24.23	12.61	*P* <0.003	*P* <0.001	*P* <0.001
PRPF19	chr11:606 70992	Chr19:109 05776	Exon	**2.04**	21.03	44.79	*P* <0.0001	*P* <0.0001	*P* <0.003
RASAL3	chr19:155 68360	chr17:323 92415	Exon	**0.90**	24.58	14.17	*P* <0.05	*P* <0.0001	*P* <0.0001
		chr17:323 92416	Exon		25.96	10.81	*P* <0.0001	*P* <0.0001	*P* <0.0001
		chr17:323 92421	Exon		23.31	14.72	*P* <0.005	*P* <0.0001	*P* <0.0001
		chr17:323 92422	Exon		24.82	8.99	*P* <0.005	*P* <0.0001	*P* <0.0001
		chr17:323 92435	Exon		27.60	6.75	*P* <0.005	*P* <0.0001	*P* <0.0001
SH3PXD2A	chr10:105 421249	Chr19:473 02650	Intron	**5.87**	32.67	8.68	*P* <0.0001	ns	*P* <0.002

Gene	Chr. Human	Chr. Mouse	Genomic Location	Methylation % Increase In Obesity (Human)	Methylation % Increase In Obesity (Obese Mouse)	Methylation % Increase In Obesity (FOb Mouse)	Human Non-Obese vs. Mouse Control	Human Obese vs. Mouse Obese	Human Obese vs. Mouse FOb
	chr10:105 451802		Intron	**4.10**			$P<0.05$	$P<0.0001$	ns
SMYD3	chr1:2459 51603	Chr1:1794 43579	Intron	**3.58**	31.84	2.44	$P<0.001$	ns	$P<0.0001$

Abbreviations: chr, chromosome; ns, not significant. Differences in methylation calculated by taking the average DNA methylation for obese and subtracting the average DNA methylation for non-obese (women) or control (mice). Statistical significance calculated by one-way ANOVA.